# Nanoceria-PAN Composite-Based Advanced Sorbent Material: A Major Step Forward in the Field of Clinical-Grade $^{68}$Ge/$^{68}$Ga Generator

**Rubel Chakravarty,[†] Rakesh Shukla,[‡] Ramu Ram, Meera Venkatesh,[†] Ashutosh Dash,*[,†] and A. K. Tyagi*[,‡]**

Radiopharmaceuticals Division, Chemistry Division, Bhabha Atomic Research Centre, Mumbai 400085, India

**ABSTRACT** The $^{68}$Ge/$^{68}$Ga generator has high potential for clinical positron emission tomography (PET) imaging. However, because of the unavailability of a suitable sorbent material, the commercially available $^{68}$Ge/$^{68}$Ga generators are not directly adaptable for the preparation of $^{68}$Ga-labeled radiopharmaceuticals. In view of this, a new nanoceria-polyacrylonitrile (PAN) composite sorbent has been synthesized by decomposition of a cerium oxalate precursor to cerium oxide and its subsequent incorporation in PAN matrix for the development of a clinical grade $^{68}$Ge/$^{68}$Ga generator. The X-ray diffraction (XRD) studies and BET nitrogen adsorption technique revealed that nanocrystalline ceria had an average particle size of ~10 nm, surface area of 72 ± 3 m$^2$/g and an average pore size of 3.8 ± 0.1 Å. Investigation of the distribution ratio ($K_d$) values for the prepared sorbent in 0.01 N HCl medium revealed the suitability of the sorbent for the quantitative retention of $^{68}$Ge and efficient elution of clinical grade $^{68}$Ga. A 370 MBq (10 mCi) $^{68}$Ge/$^{68}$Ga chromatographic generator was developed using this sorbent. $^{68}$Ga could be regularly eluted from this generator with >80% elution yield. The eluted $^{68}$Ga possess high radionuclidic purity (<1 × 10$^{-5}$% of $^{68}$Ge impurity), chemical purity (<0.1 ppm of Ce, Fe and Mn ions) and was amenable for the preparation of $^{68}$Ga-labeled radiopharmaceuticals. The generator gave a consistent performance with respect to the elution yield and purity of $^{68}$Ga over an extended period of 7 months.

**KEYWORDS:** nanocrystalline • ceria • nanocomposite • biomaterial • radiopharmaceuticals

## INTRODUCTION

Gallium-68 ($^{68}$Ga) is an excellent positron emitting radioisotope suitable for clinical positron emission tomography (PET) applications in nuclear medicine (1, 2). The relatively short half-life of $^{68}$Ga ($t_{1/2}$ = 68 min) matches the pharmacokinetics of many peptides and other biomolecules. The cyclotron independent availability of $^{68}$Ga from a $^{68}$Ge/$^{68}$Ga generator at a reasonable cost makes it an attractive and realistic option for countries with limited or no cyclotron facilities. Though several $^{68}$Ge/$^{68}$Ga generators have been reported (3–8) in the past, their direct application in a clinical context could not be accomplished, primarily because of the unavailability of suitable sorbent materials. The $^{68}$Ga solution eluted from these generators was contaminated with residuals of matrix materials (such as $TiO_2$, $SnO_2$, Ti, and Sn ions) and other cations (such as Fe, Mn, etc.) (9). The presence of these impurities in the $^{68}$Ga solution was a major obstacle in labeling receptor-specific biomolecules (9). Moreover, $^{68}$Ga was eluted with low specific volume and contained significant amounts of long-lived $^{68}$Ge ($t_{1/2}$ = 279 d) as a radionuclidic impurity (9–11). Therefore, the primary eluate did not provide sufficiently pure $^{68}$Ga for both high labeling yield and high specific activity when nanomolar amounts of peptide precursors were used (9). The $^{68}$Ga eluate could only be used for radiopharmaceutical applications after tedious multiple post-elution processing steps (9–11). Thus, it was observed that conventional first generation sorbent materials (mainly oxides of Ti and Sn) were major limiting factors to prepare clinical grade $^{68}$Ge/$^{68}$Ga generators for widespread use in routine nuclear medicine practices (9, 12–14). Hence, there is a need for a second-generation sorbent material capable of circumventing these problems so as to make this generator available for clinical applications (15).

In the quest for a second-generation sorbent material possessing high sorption capacity and selectivity for $^{68}$Ge with appreciable radiation resistance and chemical stability in acidic medium, we have made an attempt to use nanoparticle-based sorbent. It is expected that use of such materials can minimize the number of steps involved in obtaining clinical grade $^{68}$Ga from $^{68}$Ge. Several favorable characteristics, such as high surface area, availability of reactive surface sites, and pore structure make nanoparticles excellent sorbent for generator preparation (16–18). In general, nanocrystalline materials contain a large fraction of grain boundaries, which can annihilate defects, and hence such materials are more radiation-tolerant than their bulk counterparts with larger grain sizes (19, 20).

To utilize the potential of nanomaterials as a sorbent in the relatively unexplored field, our group successfully demonstrated the use of nanocrystalline titania and zirconia as prospective sorbent materials for $^{99}$Mo/$^{99m}$Tc and $^{188}$W/$^{188}$Re

* Corresponding author. E-mail: adash@barc.gov.in (A.D.); aktyagi@barc.gov.in (A.K.T.). Tel:+91-22-25595372 (A.D.); +91-22-25595330 (A.K.T.). Fax: +91-22-25505151 (A.D.); +91-22-25505151 (A.K.T.).
Received for review April 13, 2010 and accepted June 8, 2010
[†] Radiopharmaceuticals Division, Bhabha Atomic Research Centre.
[‡] Chemistry Division, Bhabha Atomic Research Centre.
DOI: 10.1021/am100325s

generators (16–18). Herein, we report a novel nanocrystalline ceria-polyacrylonitrile (PAN) composite and its use to develop a clinical grade $^{68}$Ge/$^{68}$Ga generator, for the first time. The performance of the sorbent as a column matrix for $^{68}$Ge/$^{68}$Ga generator, the yield and purity of the $^{68}$Ga obtained from the generator for the preparation of radiopharmaceuticals, have been investigated.

## EXPERIMENTAL SECTION

**Synthesis.** Cerium oxalate was precipitated by dropwise addition of 1 N oxalic acid solution (+99.9%, A.R. grade, B.D.H., India) to 0.6 N cerium(III) nitrate (+99.9%, A.R. grade, B.D.H., India) solution in 80% iso-propyl alcohol-20% deionized water (from a Millipor Milli-Q system, resistivity ~18 MΩ cm) medium. The precipitate was thoroughly washed with deionized water and dried under an infrared (IR) lamp for 1 h. The residue obtained was directly introduced in the furnace at 500 °C and calcined for 30 min in static air.

A weighed amount (1 g) of PAN (+99.9%, A.R. grade, Aldrich, England) was dissolved in 25 mL of 10 M $HNO_3$ with mild heating (~70 °C) and continuous stirring, until a viscous solution was obtained. An equal amount (1 g) of calcined cerium oxide (in 1:1 mass ratio) was added to the PAN solution with vigorous stirring to obtain homogeneous suspension of the composite. The homogeneous suspension thus formed was poured into a water bath containing 1 L of deionized water, resulting in the formation of a lump. The lump obtained was washed several times with deionized water and dried for 12 h at 70 °C in a furnace. The dried lump was crushed mechanically and sieved to obtain the particles of 50−100 mesh size (149−297 $\mu$m).

**Structural Characterization of the Sorbent.** ***X-ray Diffraction.*** X-ray diffraction data were collected on the powder sample for the phase identification and crystallite size estimation, using monochromatized Cu−Kα radiation on a PANalytical X-ray diffractometer (X'pert PRO). The instrument was operated at 40 kV and 30 mA. Silicon was used as an external standard for the correction due to instrumental line broadening. The ceria powder was ground and loaded in the groove of the perspex sample holder. XRD pattern was recorded in the $2\theta$ range of 10−90° for 1 h with a scan step size of 0.02°.

***Surface Area Measurement.*** The surface area and the pore size analysis were carried out by nitrogen adsorption (BET) technique (21) at 77 K using Quantachrome, Autosorb-1 analyzer (Quantachrome Instruments, FL 33426 USA). The nanoceria was first preheated in vacuum at 300 °C for 1 h to activate the sample.

***Transmission Electron Microscopy.*** TEM data were recorded using TEM, using a JEOL FX microscope (Jeol Ltd., Tokyo, Japan), on the powder sample. The preparation of samples for TEM analysis involved sonication in ethanol for 5 min and deposition on a carbon-coated copper grid. The accelerating voltage of the electron beam was 200 kV.

***Dynamic Light Scattering.*** The extent and nature of agglomeration were studied by particle size analyzer (Horiba, model LA-500, Japan) based on laser scattering technique. Powder sample and nonionic dispersant (Triton X 100) were initially added to deionized water for facilitating the dispersion. The suspension thus obtained was sonicated and used for the laser scattering experiments.

**Chemical Stability of Nanoceria-PAN Composite.** The chemical stability of the sorbent was assessed in mineral acids such as HCl, $HNO_3$, and $H_2SO_4$ up to concentration of 2 M. The dried sorbent (1 g) was immersed in 50 mL of solution in a stoppered conical flask for 24 h at room temperature, under continuous shaking using a wrist action shaking machine (Scientific Engineering Corporation, New Delhi, India). Subsequently, the solution was filtered and the level of Ce ions in the filtrate was determined by inductively coupled plasma-atomic emission spectroscopy (ICP-ES JY-238, Emission Horiba Group, France). The calibration curve for Ce ions was obtained by using standard solutions having known concentration of Ce ions.

**Sorption Characteristics of Nanoceria-PAN Composite.** The distribution ratios ($K_d$) of the Ge and Ga, static and dynamic sorption capacity of the sorbent were determined as per the reported procedure (16–18). To study the time dependence of $^{68}$Ge sorption on the nanoceria-PAN composite sorbent, we determined the $K_d$ of $^{68}$Ge in 0.001 M HCl at different time intervals. The $K_d$ values were taken as an indication of the progress of the adsorption process. The attainment of equilibrium was indicated by the constant $K_d$ value after a certain duration of time. The activity of $^{68}$Ge and $^{68}$Ga were determined using a HPGe detector coupled with a multichannel analyzer (MCA) (Canberra Eurisys, France) having a 1.5 keV resolution at 1333 keV and range from 1.8 keV to 2 MeV. The radioisotope levels were determined by quantification of the 511 and 1077 keV photo peaks. In all the cases, the radioactivity of $^{68}$Ge was measured after allowing the samples to decay for 2 days, whereas the radioactivity of $^{68}$Ga was measured immediately after the experiment.

**Development of $^{68}$Ge/$^{68}$Ga Generator.** To fabricate a $^{68}$Ge/$^{68}$Ga generator, we packed a borosilicate glass column of dimension 15 cm ×0.4 cm (i.d.) with a sintered disk ($G_2$) at the bottom with 0.5 g of the sorbent, in a lead shield. It was then conditioned at pH 3 by passing 100 mL of 0.001 M HCl solution, at a flow rate of 2 mL/min. The loading solution (20 mL) containing 370 MBq (10 mCi) of $^{68}$Ge solution maintained at pH 3 was allowed to percolate into the column at a flow rate of 0.25 mL/min. The column was then washed with 10 column volumes of 0.01 M HCl (pH 2) solution. The generator was regularly eluted with 0.01 M HCl solution. The generator elution profile was studied by collecting the eluate as 1 mL aliquots, and the activity of each fraction was determined by measuring the 1077 keV $\gamma$-ray peak in a HPGe detector.

**Quality Control of $^{68}$Ga for Biomedical Applications.** The radionuclidic purity of $^{68}$Ga was estimated by $\gamma$-ray spectrometry. To determine the presence of Ce, Fe and Mn ions in the $^{68}$Ga eluate as chemical impurities, the $^{68}$Ga samples were allowed to decay for 7 days. The trace levels of Ce, Fe, and Mn ions contamination in the decayed samples were determined by ICP-AES analysis. The calibration curve for Ce, Fe, and Mn ions were obtained by using standard solutions having known concentration of these ions. The presence of trace amounts organic residue from the polyacrylonitrile binding matrix was assayed by UV−visible spectrometry (JASCO V-530, UV/vis Spectrophotometer) using the decayed $^{68}$Ga samples.

$^{68}$Ga-DOTA-TATE (DOTA-D-Phe$^1$-Tyr$^3$-octreotate, DOTA = 1,4,7,10- tetraazacyclododecane-1,4,7,10-tetraacetic acid) was prepared by the reaction of 25 $\mu$g of DOTA-TATE (17.41 nmol) with $^{68}$Ga solution obtained in 0.01 M HCl medium. For the preparation of $^{68}$Ga-DOTA-TATE, 25 $\mu$L of DOTA-TATE solution in deionized water (concentration 1 $\mu$g/$\mu$L) was mixed with 475 $\mu$L of 0.1 M ammonium acetate buffer (pH ~5.5). $^{68}$Ga solution (equivalent to 185 MBq, 5 mCi) was added to the above solution and the resulting reaction mixture was incubated at 90 °C for 15 min after carefully adjusting its pH to ~5. The yield of complexation achieved was determined by reported standard procedures (22, 23) adopting paper chromatography (PC) technique as well as by high-performance liquid chromatography (HPLC). The HPLC instrument (JASCO PU 1580, Japan) was equipped with a NaI (Tl) detector. For the PC studies, 50% acetonitrile in water was used as the eluting solvent. HPLC was carried out using a dual-pump HPLC unit with a C-18 reversed phase HiQ-Sil (5 $\mu$m, 25 × 0.46 cm) column. The elution was monitored by measuring the 511 keV $\gamma$-ray of $^{68}$Ga using NaI (Tl) detector. The mobile phase consisted of water (A) and

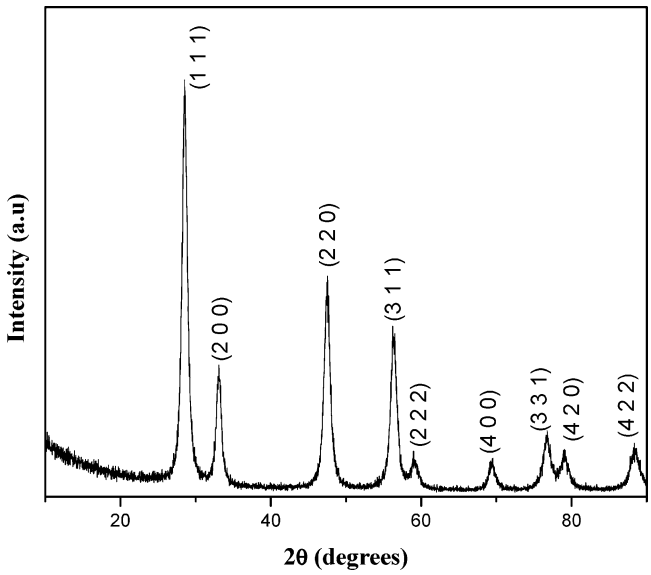


**FIGURE 1. XRD pattern of nanoceria; broadening of the peaks shows that the material is nanocrystalline.**

acetonitrile (B) mixtures with 0.1% trifluoroacetic acid and following gradient elution technique was adopted for the separation: 0−4 min 95% A, 4−15 min 95% to 5% A, 15−20 min 5% A, 20−25 min 5% A to 95% A, 25−30 min 95% A. The flow rate was maintained at 1 mL/min.

## RESULTS AND DISCUSSION

**Synthesis and Structural Characterization of the Sorbent.** Among the various synthetic strategies reported for obtaining nanocrystalline ceria (24–27), the simple precipitation route is facile to obtain $CeO_2$ nanoparticles, because of its low-cost, mild synthesis conditions and amenability for scale-up. We adopted the indirect precipitation technique in which cerium oxalate was precipitated from cerium(III) nitrate solution in isopropyl alcohol medium. The cerium oxalate precipitate was decomposed at 500 °C to obtain nanocrystalline $CeO_2$. Thermal decomposition of the oxalate material accompanied by evolution of gases increases the porosity of this material. The nanopowders obtained from this method are suitable for column chromatographic applications because of the presence of hard agglomerates and high surface area (16–18).

The structural characterization of the material was carried out using various analytical techniques like XRD, BET surface area analysis, TEM, etc. The XRD pattern (Figure 1) of the material revealed that it was nanocrystalline. The average crystallite size of nanoceria was found to be ~10 nm, which was calculated from the full width at half-maximum of the (1 1 1) peak using Scherrer's equation

$$D = \frac{0.9\lambda}{B\cos\theta_{max}}$$

where $D$ is the average crystallite size in Å, $\lambda$ is the characteristic wavelength of X-ray used (1.5406 Å), $2\theta$ is the diffraction angle, and $B$ is the angular width in radian at an intensity equal to half of the maximum peak intensity after correcting it for instrumental line broadening. The surface area of the nanocrystalline ceria was found to be $72 \pm 3$ $m^2/g$, with an average pore size of $3.8 \pm 0.1$ Å (for 5 different batches). The TEM micrograph indicated that the powder was nanocrystalline and highly agglomerated (Figure 2). The average particle size of nanocrystalline ceria as determined from the TEM micrograph (Figure 2) was found to be in the range of 8−10 nm, which is in good agreement with the results obtained from XRD.

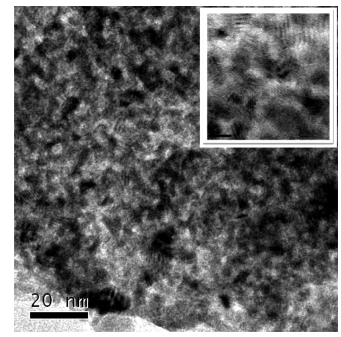


**FIGURE 2. TEM micrograph of nanoceria showing that the material is nanocrystalline and highly agglomerated.**

It was observed that although the ceria in nano form had high sorption characteristics, it was not amenable for use as a column matrix because of low permeability to aqueous liquids. To use nanoceria for column applications, a suitable binding agent was required, which would improve the granulometric properties and flow characteristics of the sorbent material (28–30). PAN was selected for this purpose because of its favorable features such as strong adhesive force with inorganic materials, high hydrophilicity, and excellent chemical stability in acidic and radiation environments (28–31).

PAN has been shown to effectively immobilize ion-exchange materials into granular forms, without altering the sorption behavior of these materials (28–30). The PAN granules obtained by dispersing PAN solution in water are highly porous (28–30, 32). The pores of these granules are mainly (>99.9%) composed of macropores (pore size >0.05 $\mu$m) along with a minor portion (<0.1%) of mesopores (pore size between 0.002 and 0.05 $\mu$m) (32). When the ion exchanger is mixed with the PAN solution and dispersed in water, the resultant PAN granules obtained can accommodate very high loadings of the ion exchange material (up to 90% by weight) into the PAN matrix (28–32). These porous PAN granules exhibit numerous advantages over other sorbents such as improved kinetics, enhanced sorption capacity due to the increased availability of the sorbent material, easy modification of physicochemical properties (hydrophilicity, porosity, mechanical strength), and simplified production (28–30).

The particle size distribution of the calcined nanoceria and nanoceria-PAN composite were studied by a particle size analyzer based on laser scattering. The success of the technique depends on dispersion of the powder in a solvent. Because the synthesized powders are essentially agglomerates of primary nanoparticles, it is difficult to disperse them as individual particles. Moreover, because of instrumental

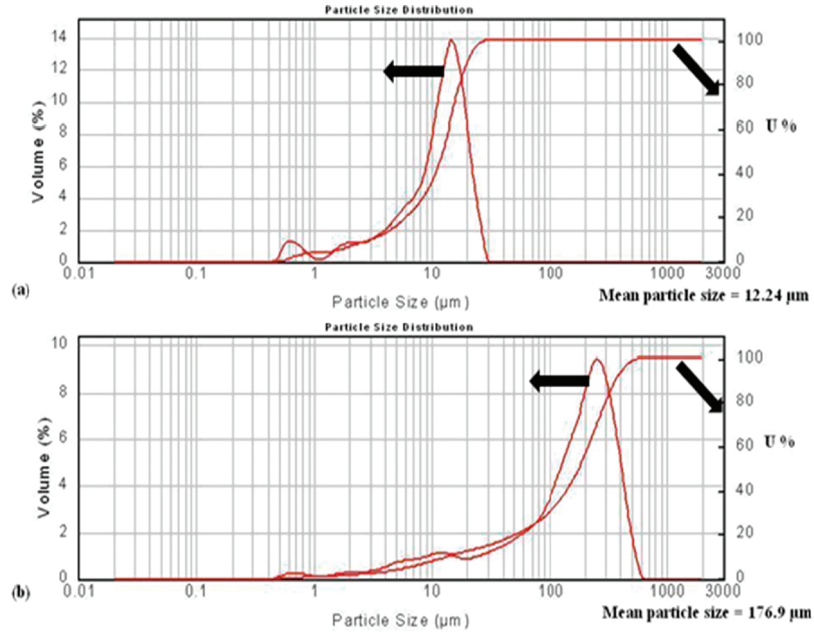


**FIGURE 3. Particle size distribution for (a) ceria nanopowder and (b) nanoceria-PAN composite. Volume number distribution (in %) versus particle size (log form) is plotted on the left-hand side of the graph. On right-hand side, U% (percentage of the total number of particles under the given size) versus particle size (log form) is shown**

limitation, this technique is unable to provide the true size of the primary nanoparticles. However, it is a good tool to find out the size and nature of the agglomerates. Ultrasonication was used to make dispersion of the nano powder in the deionized water. Dynamic light scattering results of nanoceria powder and nanoceria-PAN composite are shown in Figure 3. Volume number distribution (in %) versus particle size (log form) is plotted on the left-hand side of the graph. On the right-hand side, U% (percentage of the total number of particles under the given size) versus particle size (log form) is shown. The mean particle size of the nanoceria and the nanoceria-PAN composite was found to be 12.24 and 176.9 $\mu$m, respectively. Thus it can be inferred that the mean agglomerate size increases after binding nanoceria with PAN. However, the XRD pattern of nanoceria remains unchanged on binding with PAN.

**Chemical Stability of Nanoceria-PAN Composite.** The chemical stability studies by solubility tests showed that the composite sorbent was insoluble in water and dilute mineral acids as negligible amount of Ce ions (<0.1 ppm) were detected in the filtrate when analyzed by ICP-AES. The unparalleled chemostability of cerium oxide in these solvents ensures that it does not lead to any added chemical impurities in the eluate.

**Sorption Characteristics of Nanoceria-PAN Composite.** The results (summarized in Table 1) indicated that the $K_d$ values vary with the concentration of the contact medium. Ge has significantly high distribution ratio ($K_d$), which decreases gradually with an increase in concentration of HCl. On the other hand, $^{68}$Ga has a remarkably lower distribution ratio ($K_d$) and can thus be effectively separated from parent $^{68}$Ge. In the design of an adsorption column, it is essential to retain $^{68}$Ge quantitatively on the sorbent matrix which was the case at 0.001 M HCl owing to high distribution ratio ($K_d$) of $^{68}$Ge at this concentration. As indicated from the results of distribution ratio ($K_d$) values, $^{68}$Ga formed from the decay of $^{68}$Ge was not at all retained by the sorbent matrix at 0.01 M HCl solution and hence could be eluted out easily. Nanocrystalline ceria particles can be considered to consist of isolated cerium oxide clusters which on interaction with aqueous solution results in the hydroxylation of surface active sites and in turn a pH-dependent positive surface charge is imparted, which is primarily responsible for the uptake of corresponding metal ions. In acid solutions (pH 1−3) the principal germanium species (33, 34) are $[GeO(OH)_5]^-$, $[GeO_2(OH)_2]^{2-}$, and $[[Ge(OH)_4]_8(OH)_3]^{3-}$, which are negatively charged. The strong affinity of $^{68}$Ge on the nanoceria sorbent in this pH range is attributed to the electrostatic interaction of negatively charged germanium species with the positively charged surface of the sorbent. In the same medium, Ga exists as $Ga^{3+}$ ions and hence a nearly complete elution could be achieved because of absence of electrostatic interaction due to the same type of charges.

**Table 1. Distribution Ratios ($K_d$) of $^{68}$Ge and $^{68}$Ga**

| | $K_d$ | |
|---|---|---|
| conc. of HCl(M) | $^{68}$Ge | $^{68}$Ga |
| 0.001 | 5233 | 113 |
| 0.01 | 5152 | 0.1 |
| 0.05 | 4766 | 0.2 |
| 0.1 | 3033 | 0.3 |
| 0.5 | 2109 | 0.5 |
| 1 | 1654 | 0.6 |
| 2 | 1636 | 0.7 |
| 3 | 837 | 0.6 |
| 4 | 414 | 0.7 |
| 5 | 342 | 0.7 |

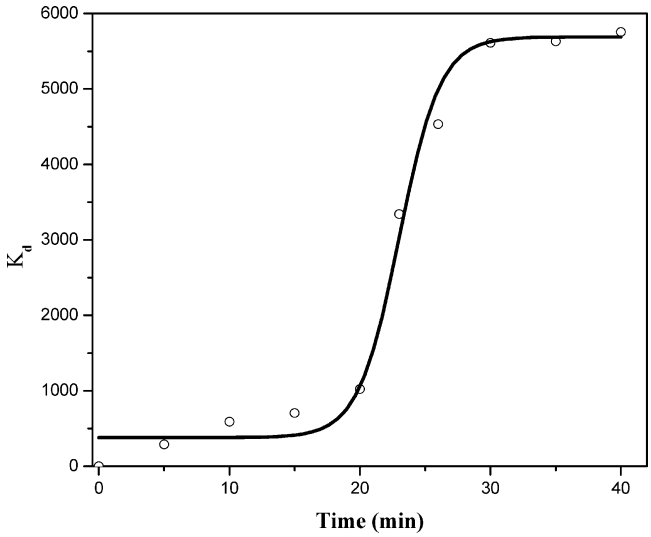


FIGURE 4. Determination of equilibration time as indicated by the constant $K_d$ value of $^{68}$Ge.

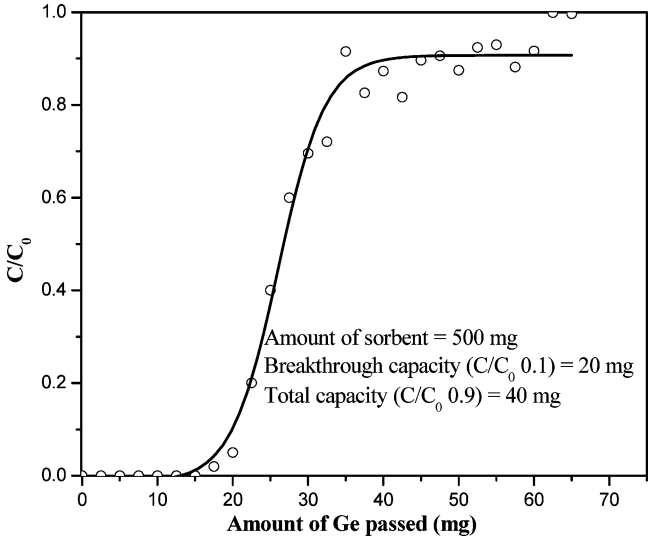


FIGURE 5. Breakthrough profile of nanoceria column when Ge solution (at pH 3) was passed through the column at a flow rate of 0.25 mL/min.

To determine the time required to attain equilibrium, we measured the time dependence of the sorption of $^{68}$Ge ions on the sorbent and the result is depicted in Figure 4. As inferred from the curve, the equilibrium was attained within 25−30 min and therefore a contact period of ~30 min was maintained for all the batch experiments. The results of the capacity determination experiment by batch equilibrium method indicated that the mean capacity value (in 10 different batches) of the nano composite sorbent for Ge was 40 ± 5 mg/g at pH 3. The sorption capacity of nanoceria-PAN composite was ~20 times higher than that of the bulk ceria (~2 mg/g). In order to study the sorption behavior of $^{68}$Ge in generator column bed containing the composite sorbent, the breakthrough profile (Figure 5) was studied at pH ~3. It was observed that after retention of (20 ± 2) mg of Ge per g of sorbent ($n$ = 10) in the column, the breakthrough point was reached. These results reflect that even a small column containing 200 mg of the sorbent is adequate for the preparation of a 3.7 GBq (100 mCi) generator. In the

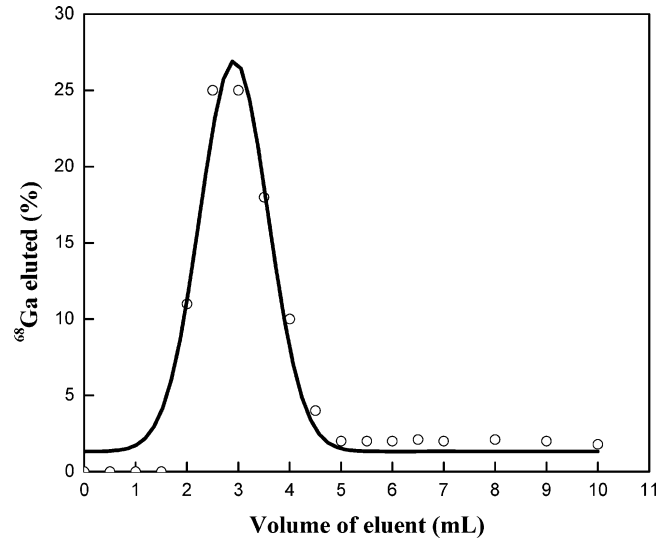


FIGURE 6. Elution profile of the generator on eluting $^{68}$Ga with 0.01 M HCl at a flow rate of 1 mL/min.

nanosized cerium oxide particles, the sorption sites are predominantly located on the surface and offer high sorption capacity per unit mass, because of the high surface area-to-volume ratio.

**Development of $^{68}$Ge/$^{68}$Ga Generator.** The separation process could be demonstrated by developing a 370 MBq (10 mCi) $^{68}$Ge/$^{68}$Ga generator. To optimize the minimum volume of eluent required for the elution of $^{68}$Ga with maximum yield and radioactive concentration, we studied the elution profile of the generator (Figure 6). It is evident from the elution curve that >95% of the $^{68}$Ga activity could be eluted in an ionic form using a small volume (3 mL) of 0.01 M HCl, with appreciable radioactive concentration, thereby avoiding the post-elution concentration step. The present generator has been giving a consistent yield (82 ± 5%) of $^{68}$Ga for the past 7 months and is still performing well without any degradation in the performance. The major advantage of this generator is its consistency, which is far superior to that of the presently used generators, which show degrading performance on repeated elution, over a prolonged period of time (6, 14, 23, 35).

**Quality Control of $^{68}$Ga for Biomedical Applications.** The eluted $^{68}$Ga is intended to be used for human applications and therefore stringent quality control measures are required to estimate the level of long-lived $^{68}$Ge impurity present in it. Because $^{68}$Ge decays solely by electron capture to $^{68}$Ga, the amount of $^{68}$Ge contamination in $^{68}$Ga eluate could not be directly estimated by $\gamma$-ray spectrometry. The $^{68}$Ge contamination level in $^{68}$Ga was quantified by allowing the separated $^{68}$Ga samples to decay for 24 h and then measuring the 511 keV $\gamma$-ray peak, corresponding to emission from $^{68}$Ga daughter. This in turn corresponds to the level of $^{68}$Ge contaminant, which exists in secular equilibrium with $^{68}$Ga. The amount of $^{68}$Ge impurity in $^{68}$Ga eluate was <20 Bq (<$10^{-5}$% of the total $^{68}$Ga activity) in all the elutions over the period of 7 months. The radionuclidic purity of $^{68}$Ga obtained from this generator is comparable to that obtained from commercial generators (9, 14). How-

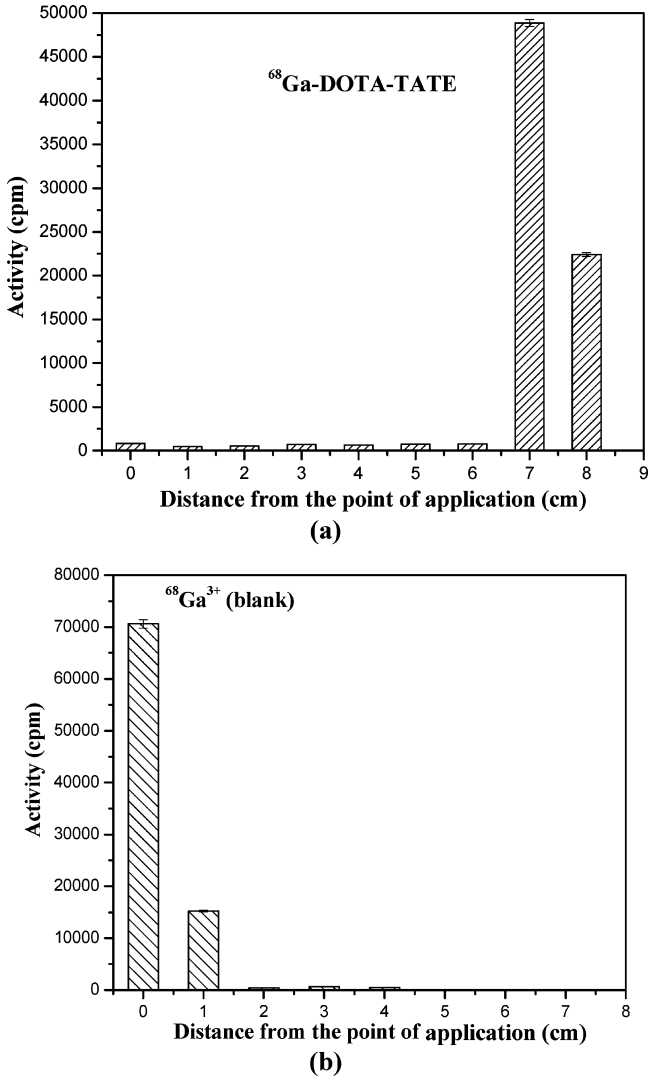


**FIGURE 7. Paper chromatographic patterns of (a) $^{68}$Ga-DOTA-TATE and (b) $^{68}$Ga$^{3+}$ (blank) using 50% acetonitrile in water as the eluting solvent.**

ever, the eluate ($^{68}$Ga) from commercial generators were subjected to multiple purification steps (9, 14) to obtain clinical grade $^{68}$Ga, whereas, the reported method provides $^{68}$Ga of similar purity in a single step. This proves that $^{68}$Ga is obtained with high radionuclidic purity, which is suitable for radiopharmaceutical applications. The chemical impurities present in the $^{68}$Ga eluate in the form of Ce, Fe, and Mn ions were <0.1 mg/L (0.1 ppm), as ascertained by ICP-AES analyses of the decayed samples. It is reported that PAN shows weak absorption at $\lambda_{max}$ of 278 nm in the UV−visible spectra, which corresponds to the n−$\pi$* transition of nitrile-groups (36). From the UV−visible spectra of the decayed $^{68}$Ga samples, it could be inferred that PAN residue was not present in the $^{68}$Ga eluate, as no absorption was observed at this wavelength.

The suitability of $^{68}$Ga eluted from the generator for biomedical applications could be demonstrated by labeling DOTA-TATE (in nanomolar concentrations) with $^{68}$Ga. $^{68}$Ga-DOTA-TATE is a radiopharmaceutical presently being used for the PET imaging of in operable neuro endocrine tumors overexpressing somatostatin receptors. The radiolabeling of DOTA-TATE with $^{68}$Ga is also an indirect test to ascertain the chemical purity of $^{68}$Ga as very high chemical purity is essential to achieve a good complexation yield of the radio-labeled agent. The complexation yield was determined by paper chromatography (PC) using 50% acetonitrile in water as eluent and it was observed that $^{68}$Ga-DOTA-TATE moved toward the solvent front ($R_f = 0.8-0.9$) (Figure 7a), whereas under identical conditions, unlabeled $^{68}$Ga$^{3+}$ remained at the point of spotting ($R_f = 0$) (Figure 7b). The complexation yield of $^{68}$Ga-DOTA-TATE was also validated by HPLC studies. The typical HPLC pattern of $^{68}$Ga-DOTA-TATE prepared under the optimized conditions is shown in Figure 8. From PC studies, it was observed that 25 $\mu$g of DOTA-TATE (17.41 nmol) was sufficient for labeling ~185 MBq (5 mCi) of $^{68}$Ga with >99% complexation yield. The specific activity of $^{68}$Ga-DOTA-TATE was ~10.6 MBq/nmol and it was obtained with >99% radiochemical purity. The high radiochemical purity of $^{68}$Ga-DOTA-TATE was comparable to that of $^{68}$Ga-DOTA-peptides prepared by the reported methods adopting multiple purification steps (9, 23, 37, 38). This proves that the $^{68}$Ga eluted from the generator was suitable for preparing PET imaging agents, with adequate purity as well as specific activity for clinical applications.

It has been reported that PAN-based composite ion-exchangers exhibit excellent radiation stability in aqueous acidic solutions up to a radiation dose of $1 \times 10^6$ Gy, with no negative effect on sorption properties at this dose (28–30, 39). Though the consistency of the elution yield (>80%) and purity of $^{68}$Ga are a good indication of the radiation stability of the composite sorbent, the effect of radiation at higher level of activity is yet to be demonstrated. Further investigations are warranted to establish the useful-

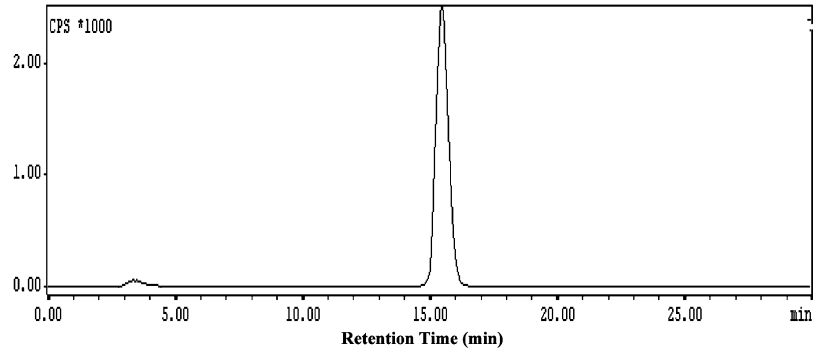


**FIGURE 8. HPLC pattern of $^{68}$Ga-DOTA-TATE.**

ness of this sorbent for the preparation of a clinical size generator (50−100 mCi or 1.85−3.7 GBq). However, the present findings suggest that this material holds promise to be a useful sorbent for the preparation of $^{68}$Ge/$^{68}$Ga generator. The radiation stability of the sorbent at higher radiation doses is planned to be studied separately. Although the radiochemical as well as radionuclidic purity of $^{68}$Ga were evaluated, the biological purity in terms of sterility and absence of bacterial endotoxins for formulation of $^{68}$Ga radiopharmaceuticals need to be addressed in the next step.

Several modifications can be incorporated in this new generator system developed by us. This includes scaling up to higher activity level (up to 3.7 GBq, 100 mCi), use of extremely high purity reagents to avoid metal ion contamination, obtaining the $^{68}$Ga eluate in a sterile form by passing it through 0.22 $\mu$m sterile filter (23) and automation of the entire process. It is our goal to carry out all these developments in the near future to improve this generator into an easily adaptable system for hospital radiopharmacies.

## CONCLUSIONS

In summary, a potential pathway to rationally synthesize a new composite sorbent nanoceria-PAN suitable for the preparation of a clinical grade $^{68}$Ge/$^{68}$Ga generator has been established. The efficacy of this second-generation advanced sorbent material could be demonstrated by developing a 370 MBq (10 mCi) $^{68}$Ge/$^{68}$Ga generator, which is still giving consistently good performance after repeated elutions over a period of 7 months. $^{68}$Ga could be regularly eluted from the generator with acceptable radioactive concentration with substantially high yield and purity. The efficacy of $^{68}$Ga for the preparation of radiopharmaceuticals for PET imaging could be confirmed by labeling DOTA-TATE with very high complexation yield. The results presented here are promising and the generator system is amenable for automation. This generator may be very useful for countries where commercial sources of PET radioisotopes are not readily available or too expensive. This study has tremendous potential to open up many new opportunities in design and studies of novel nanomaterial based composite sorbents suitable for development of other radionuclide generators for biomedical applications.

**Acknowledgment.** The authors are grateful to Prof. V. Venugopal, Director, Radiochemistry and Isotope Group, Bhabha Atomic Research Centre, for his support to this program. Thanks are due to Dr. Tapas Das and Dr. Sudipta Chakraborty, Radiopharmaceuticals Division, BARC, for their help in carrying out the radiolabeling experiments.

### REFERENCES AND NOTES

(1) Fani, M.; André, J. P.; Maecke, H. R. *Contrast Media Mol. Imaging* **2008**, *3* (2), 53–63.
(2) Pagou, M.; Zerizer, I.; Al-Nahhas, A. *Hellenic J. Nucl. Med.* **2009**, *12* (2), 102–105.
(3) Nakayama, M.; Haratake, M.; Ono, M.; Koiso, T.; Harada, K.; Nakayama, H.; Yahara, S.; Arano, Y. *Appl. Radiat. Isot.* **2003**, *58* (1), 9–14.
(4) Benhong, C.; Zongquan, L.; Yongxian, W. *J. Radioanal. Nucl. Chem.* **1998**, *238*, 175–177.
(5) Bao, B.; Song, M. *J. Radioanal. Nucl. Chem* **1996**, *213*, 233–238.
(6) McElvany, K. D.; Hopkins, K. T.; Welch, M. J. *Int. J. Appl. Radiat. Isot.* **1984**, *35*, 521–524.
(7) Waters, S. L.; Horlock, P. L.; Kensett, M. J. *Int. J. Appl. Radiat. Isot.* **1983**, *34*, 1023.
(8) Arino, H.; Skraba, W. J.; Kramer, H. H. *Int. J. Appl. Radiat. Isot.* **1978**, *29*, 117–120.
(9) Zhernosekov, K. P.; Filosofov, D. V.; Baum, R. P.; Aschoff, P.; Bihl, H.; Razbash, A. A.; Jahn, M.; Rösch, F. *J. Nucl. Med.* **2007**, *48*, 1741–1748.
(10) Gebhardt, P.; Opfermann, Th.; Saluz, H. P. *Appl. Radiat. Isot.* **2010**, in press.
(11) Aardaneh, K.; Van Der Walt, T. N. *J. Radioanal. Nucl. Chem.* **2006**, *268*, 25–32.
(12) Breeman, W. A. P.; Verbuggen, A. M. *Eur. J. Nucl. Med. Mol. Imaging* **2007**, *34*, 978–981.
(13) Velikyan, I.; Beyer, G. J.; Langstrom, B. *Bioconjugate Chem.* **2004**, *15*, 554–60.
(14) Asti, M.; Pietri, G. D.; Fraternali, A.; Grassi, E.; Sghedoni, R.; Fioroni, F.; Roesch, F.; Versari, A.; Salvo, D. *Nucl. Med. Biol.* **2008**, *35*, 721–724.
(15) Nakayama, M.; Haratake, M.; Ono, M.; Koiso, T.; Harada, K.; Nakayama, H.; Yahara, S.; Ohmomo, Y.; Arano, Y. *Appl. Radiat. Isot.* **2003**, *58*, 9–14.
(16) Chakravarty, R.; Shukla, R.; Ram, R.; Gandhi, S.; Dash, A.; Venkatesh, M.; Tyagi, A. K. *J. Nanosci. Nanotechnol.* **2008**, *8*, 4447–4452.
(17) Chakravarty, R.; Dash, A.; Venkatesh, M. *Chromatographia* **2009**, *69*, 1363–1371.
(18) Chakravarty, R.; Shukla, R.; Tyagi, A. K.; Dash, A.; Venkatesh, M. *Appl. Radiat. Isot.* **2010**, *68*, 229–238.
(19) Bai, X. M.; Voter, A. F.; Hoagland, R. G.; Nastasi, M.; Uberuaga, B. P. *Science* **2010**, *327*, 1631–1634.
(20) Rose, M.; Balogh, A. G.; Hahn, H. *Nucl. Instrum. Methods Phys. Res., Sect. B* **1997**, *119*, 127–128.
(21) Leofanti, G.; Padovan, M.; Tozzola, G.; Venturelli, B. *Catal. Today* **1998**, *41*, 207–219.
(22) Pierro, D. D.; Rizzello, A.; Cicoria, G.; Lodi, F.; Marengo, M.; Pancaldi, D.; Trespidi, S.; Boschi, S. *Appl. Radiat. Isot.* **2008**, *66*, 1091–1096.
(23) Decristoforo, C.; Knopp, R.; von Guggenberg, E.; Rupprich, M.; Dreger, T.; Hess, A.; Virgolini, I.; Haubner, R. *Nucl. Med. Commun.* **2007**, *28*, 870–875.
(24) Chengyun, W.; Yitai, Q.; Yi, X.; Changsui, W.; Li, Y.; Guiwen, Z. *Mater. Sci. Eng.* **1996**, *B39*, 160–162.
(25) Czerwinski, F.; Szpunar, J. A. *J. Sol-Gel Sci. Technol.* **1997**, *9*, 103–114.
(26) Shuo, S.; Runhua, L.; Taotao, W.; Haiying, S.; Hanqing, W. *J. Dispersion Sci. Technol.* **1999**, *20*, 1247–1262.
(27) Chen, H.; Chang, H. *Ceram. Int.* **2005**, *31*, 795–802.
(28) Sebesta, F. *J. Radioanal. Nucl. Chem.* **1997**, *220*, 77–88.
(29) Nilchi, A.; Khanchi, A.; Atashi, H.; Bagheri, A.; Nematollahi, L. *J. Hazard. Mater.* **2006**, *A137*, 1271–1276.
(30) Nilchi, A.; Atashi, H.; Javid, A. H.; Saberi, R. *Appl. Radiat. Isot.* **2007**, *65*, 482–487.
(31) Xue, T. J.; McKinney, A.; Wilkie, C. A. *Polym. Degrad. Stab.* **1997**, *58*, 193–202.
(32) Kim, H.; Lee, C.; Shul, Y.; Moon, J.; Lee, E. *Sep. Sci. Technol.* **2003**, *38*, 695–713.
(33) Neirinckx, A. D.; Davis, M. A. *J. Nucl. Med.* **1979**, *20*, 1075–1079.
(34) Everest, D. A.; Salmon, J. E. *J. Chem. Soc.* **1954**, 2438–2443.
(35) Mirzadeh, S.; Knapp, Jr., F. F. *J. Radioanal. Nucl. Chem.* **1996**, *203*, 471–488.
(36) Vega, I.; Morris, W.; D'Accorso, N. *React. Funct. Polym.* **2006**, *66*, 1609–1618.
(37) Azhdarinia, A.; Yang, D. J.; Chao, C.; Mourtada, F. *Nucl. Med. Biol.* **2007**, *34*, 121–127.
(38) Meyer, G.-J.; Mäcke, H.; Schuhmacher, J.; Knapp, W. H.; Hofmann, M. *Eur. J. Nucl. Med. Mol. Imaging* **2004**, *31*, 1097–1104.
(39) Sebesta, F.; John, J.; Motl, A.; Stamberg, K. *Evaluation of Polyacrylonitrile (PAN) As a Binding Polymer for Absorbers Used to Treat Liquid Radioactive Wastes*; SNL Report 95-2729; Sandia National Laboratories: Albuquerque, NM, 1995.

AM100325S